Effect of three-dimensional strain states on magnetic anisotropy of $La_{0.8}Ca_{0.2}MnO_3$ epitaxial thin films

T. K. Nath, R. A. Rao, D. Lavric, and C. B. Eom[a)]
Department of Mechanical Engineering and Materials Science, Duke University, Durham, North Carolina 27708

L. Wu and F. Tsui
Department of Physics and Astronomy, University of North Carolina, Chapel Hill, North Carolina 27599

(Received 10 November 1998; accepted for publication 18 January 1999)

Magnetic anisotropy of $La_{0.8}Ca_{0.2}MnO_3$ (LCMO) epitaxial thin films grown on (001) $SrTiO_3$ and $LaAlO_3$ a substrates exhibits strong correlation with substrate-induced strain states as determined by normal and grazing incidence x-ray diffraction. In a 250 Å thick LCMO $(001)^T$ film grown on $SrTiO_3$ substrate, an in-plane biaxial magnetic anisotropy is observed, and it is accompanied by a substrate-induced in-plane biaxial tensile strain. In contrast, the observed magnetic easy axis for a 250 Å $(110)^T$ film grown on $LaAlO_3$ substrate is perpendicular to the film plane, and the corresponding in-plane strain is biaxial compressive. In both cases the magnetic easy axes are along the crystallographic directions under tensile strain, indicating the presence of a positive magnetostriction. In thicker films (~4000 Å) grown on both substrates that are nearly strain relaxed, the magnetic easy axis lies in the film plane along the [110] direction of the (001) substrate. © *1999 American Institute of Physics.* [S0003-6951(99)01711-8]

Epitaxial thin films of rare earth manganese perovskites exhibit a variety of interesting magnetic and magnetotransport behavior, including the colossal magnetoresistance (CMR) effect.[1] These properties are often quite different from intrinsic properties of the bulk materials, and they are evidently due to epitaxial constraints. For instance, strained (110) $SrRuO_3$ single domain epitaxial thin films show uniaxial magnetic anisotropy,[2] while the bulk single crystal exhibits a biaxial anisotropy.[3] It has been shown[4–6] that substrate-induced strain plays a dominant role in magnetic anisotropy of CMR manganite epitaxial thin films. Strain-dependent properties of epitaxial manganite films are also important for many potential device applications.[7] It has been recognized[8] that it is possible to tailor magnetic anisotropy and to change three-dimensional (3D) strain states in epitaxial CMR thin films by varying film thickness and substrate type. However, 3D strain states and their influence on magnetism of epitaxial CMR manganite thin films have not yet been studied systematically.

In this letter we report a systematic study of 3D strain states and magnetic anisotropy of 250 and 4000 Å $La_{0.8}Ca_{0.2}MnO_3$ (LCMO) epitaxial thin films grown on either (001) $LaAlO_3$ (LAO) or (001) $SrTiO_3$ (STO) substrates. The LCMO films were grown using a pulsed laser deposition technique at 700 °C with an oxygen partial pressure of 400 mTorr. The lattice parameters and 3D strain states were determined by normal and grazing incidence diffraction (GID) θ–2θ scans, using a four-circle x-ray diffractometer. Magnetic measurements were carried out using a Quantum Design superconducting quantum interference device (SQUID) magnetometer. Special sample holders were used to position the samples along chosen crystallographic directions.

The bulk LCMO target is a distorted perovskite with a pseudocubic lattice parameter of $a_o^P = 3.881$ Å. The tilting of the MnO_6 octahedra results in a tetragonal structure with lattice parameters $a_o^T = b_o^T = \sqrt{2}a_o^P$ and $c_o^T = 2a_o^P$. In this letter, Miller indices are based on this tetragonal unit cell, indicated by a superscript ''*T*.'' The tetragonal distortion enables one to distinguish between the $(110)^T$ and $(001)^T$ oriented films, using off-axis azimuthal ϕ x-ray scans.[9,10] The ability to distinguish the two tetragonal orientations is crucial for the study of magnetic anisotropy in LCMO films. Detailed thickness-dependent lattice distortions of these films have been described elsewhere.[10]

Our x-ray diffraction experiments show that the LCMO thin films grown on LAO ($a_o = 3.792$ Å) substrates are under a biaxial compressive stress in the growth plane, induced by a -2.30% lattice mismatch with the substrate. In contrast, the LCMO films grown on STO ($a_o = 3.905$ Å) substrates show a biaxial tensile stress in the growth plane, which is induced by a $+0.62\%$ lattice mismatch. These are demonstrated in Fig. 1 by the normal and GID θ–2θ scans of 250 Å LCMO films grown on STO and LAO substrates. The out-of-plane and in-plane lattice parameters of the 250 Å film grown on STO are (3.855 ± 0.002) Å and (3.910 ± 0.003) Å, respectively, indicating an in-plane biaxial tensile strain with $\epsilon_{xx} = \epsilon_{yy} = 0.74\%$ and a corresponding out-of-plane uniaxial compression with $\epsilon_{zz} = -0.68\%$. In the 250 Å film grown on LAO, the respective lattice parameters are (3.917 ± 0.001) Å and (3.844 ± 0.010) Å, leading to a contrasting distortion with $\epsilon_{xx} = \epsilon_{yy} = -0.99\%$ and $\epsilon_{zz} = 0.92\%$ when compared to its STO counterpart.

Crystallographic textures can also play an important role in determining magnetic anisotropy in LCMO films. The near degeneracy of $(110)^T$ and $(001)^T$ reflections has made it impossible to distinguish the two out-of-plane textures using the normal θ–2θ scans alone. Instead, off-axis azimuthal ϕ scans of nondegenerate reflections, such as $(111)^T$, $(221)^T$, and $(113)^T$, are used to identify the texture. The 250 Å LCMO film grown on STO exhibits a pure $(001)^T$ normal texture, as illustrated in Figs. 2(a) and 2(b) by the ϕ scans of the $(111)^T$ reflection. The pure $(001)^T$ texture is indicated by

a)Electronic mail: eom@acpub.duke.edu

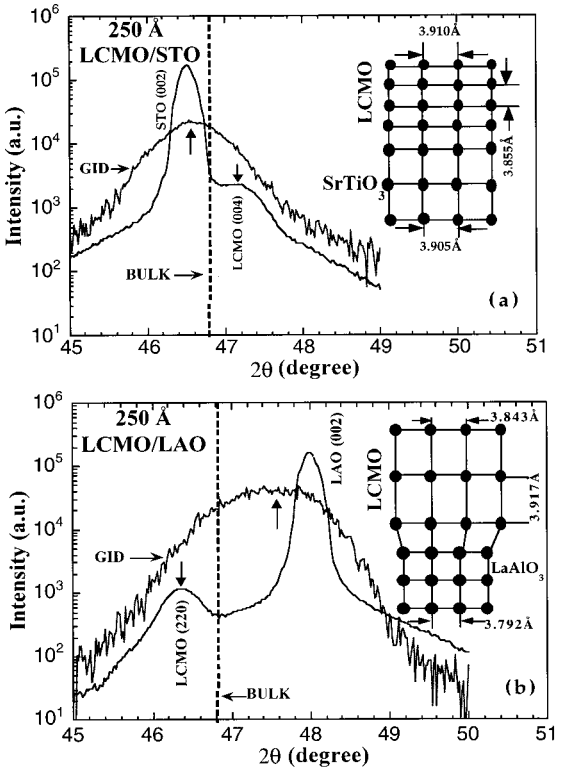

FIG. 1. X-ray normal and grazing incidence diffraction (GID) θ–2θ scans for 250 Å LCMO epitaxial films grown on (1) (001) $SrTiO_3$ and (b) (001) $LaAlO_3$ substrates. The dotted lines indicate bulk 2θ values of LCMO, and the vertical arrows indicate the film peaks. Insets: schematic diagrams of cross-sectional view of the strained lattices.

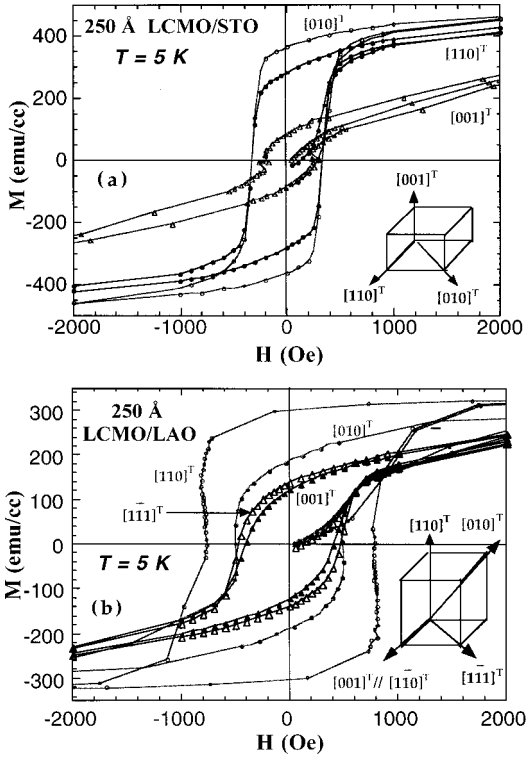

FIG. 3. Magnetic hysteresis loops at 5 K with fields applied along (a) $[010]^T$ (open circles), $[110]^T$ (closed circles), and $[100]^T$ (triangles) for a 250 Å LCMO epitaxial film grown on (001) $SrTiO_3$ substrate, and (b) $[010]^T$ (closed circles), $[110]^T$ (open circles), $[001]^T$ (closed triangles), and $[1\bar{1}1]^T$ (open triangles) for a 250 Å LCMO epitaxial film grown on (001) $LaAlO_3$ substrate.

the observed four peaks at every 90° interval along $(001)^T$ [Fig. 2(a)], and no peaks along $(110)^T$ [Fig. 2(b)]. The in-plane epitaxial arrangement deduced from the scans is LCMO $[110]^T \| SrTiO_3[100]$, and LCMO $[\bar{1}10]^T \| SrTiO_3$ $[010]$. In contrast, the corresponding $(111)^T$ ϕ scans for the 250 Å film grown on LAO indicate the presence of a pure $(110)^T$ normal texture with no $(001)^T$ oriented grains, as shown in Figs. 2(c) and 2(d). The observed four peaks shown in Fig. 2(c) indicate the presence of two orthogonal in-plane domains.

Orientation-dependent magnetic hysteresis loops were measured in order to probe the effects of magnetic anisotropy. The behavior at 5 K for the 250 Å LCMO film grown on STO is shown in Fig. 3(a). The magnetization perpendicular to the film, after it has been corrected for the demagnetization effect, exhibits a high saturation field H_s (~10 kOe) and nearly zero remanent magnetization M_r, indicating that the magnetic hard axis is along $[001]^T$ with film plane being magnetically easy. In-plane magnetization loops are nearly square, and they saturate much faster ($H_s \sim 2$ kOe). The observed saturation magnetization (M_s) is about 3.4 μ_B/Mn, and the coercive field (H_C) is about 300 Oe. The higher remanence for the behavior along $[010]^T$ (nearly equal to M_s) compared to that of the $[110]^T$ indicates that the magnetic easy axis is along the in-plane $\langle 010 \rangle^T$ directions, and that the magnetization along $[110]^T$ in zero field relaxes back to the nearest easy axis. The observed behavior corresponds to the characteristics of biaxial anisotropy. The less than 100% remanence for the easy-axis magnetization is likely to be the result of structural inhomogeneity. The observed behavior for the 250 Å LCMO film grown on LAO is entirely different, as shown in Fig. 3(b). In this case, the perpendicular magnetization loops (field along $[110]^T$) after demagnetization corrections is nearly square with a near 100% remanence and a higher H_c (~800 Oe), when compared to the in-plane behavior with $H_s \sim 8$ kOe and $H_c \sim 400$ Oe [see Fig. 3(b)]. In contrast to the film grown on STO, the observed magnetic easy axis for the film on LAO is perpendicular to film along the $[110]^T$ direction.

The observed magnetic anisotropy for the two 250 Å LCMO films exhibits strong correlation with respect to their

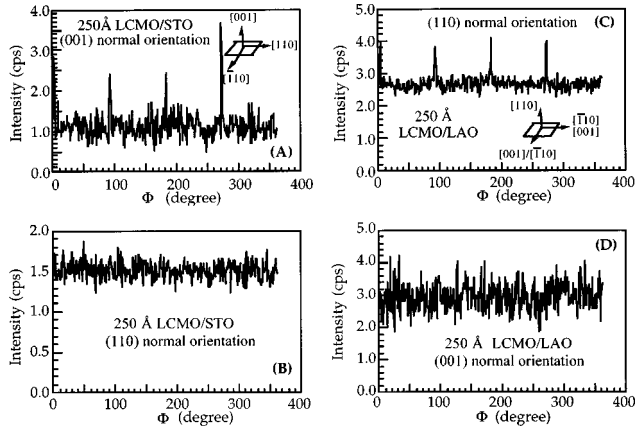

FIG. 2. Off-axis azimuthal ϕ scans of (111) reflections for a 250 Å LCMO epitaxial thin film grown on (001) $SrTiO_3$ corresponding to (a) (001) and (b) (110) normal orientations, and for a 250 Å LCMO film grown on (001) $LaAlO_3$ corresponding to (c) (110) and (d) (001) normal orientations. Insets: schematic diagrams of the crystallographic domain structures.

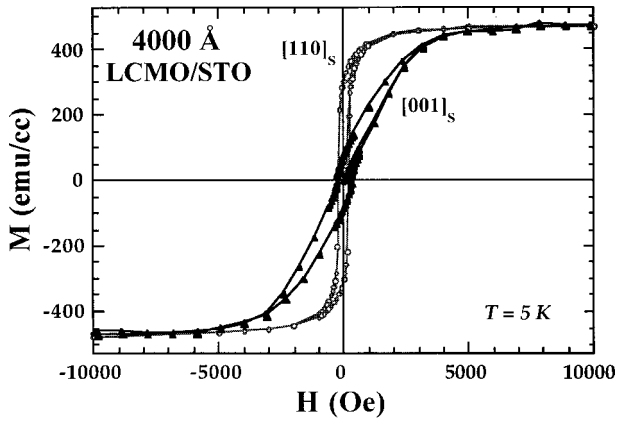

FIG. 4. Magnetic hysteresis loops at 5 K with fields applied along the in-plane $[110]_s$ of the substrate (open circles) and along the normal $[001]_s$ (closed triangles) for 4000 Å LCMO films grown on STO. The subscript "*S*" denotes Miller indices of the substrate.

3D strain states discussed above. The observed in-plane biaxial compressive stress and the corresponding out-of-plane *uniaxial* tensile strain in the film grown on LAO appear to induce the observed perpendicular *uniaxial* anisotropy, while the in-plane *biaxial* tensile stress in the film grown on STO seems to give rise to the in-plane *biaxial* anisotropy. In both cases, the magnetic easy axis is along the direction of tensile strain, indicating the presence of a positive magnetostriction in LCMO films.[11]

In order to probe the contributions of stress-induced anisotropy and the intrinsic magnetocrystalline anisotropy to the magnetic anisotropy of LCMO films, 3D strain states[10] and magnetic anisotropy of strain relaxed thick films were measured. The observed in-plane and out-of-plane lattice parameters of a 4000 Å LCMO film grown on STO are (3.8885 $\pm$0.0005) Å and (3.867$\pm$0.0007) Å, respectively. In the case of a 4000 Å film grown on LAO, the respective in-plane and out-of-plane values are (3.889$\pm$0.004) Å and (3.871$\pm$0.001) Å. The lattice parameters for both samples are very close to the bulk value, so that the effect of stress-induced anisotropy is expected to be small. However, unlike their 250 Å counterparts, the thicker films contain a mixture of $(001)^T$ and $(110)^T$ normal orientations,[10] with the amount of the former about 2/3 of the total. The observed orientation-dependent magnetization loops for the two 4000 Å LCMO films indicate that their magnetic easy axes are biaxial, along the in-plane $\langle 110\rangle$ directions of the substrate or along the $\langle 010\rangle^T$ of the $(001)^T$ texture, as shown in Fig. 4 for the behavior of the LCMO/STO sample at 5 K. In the absence of stress-induced anisotropy and in the presence of predominantly $(001)^T$ domains, it is reasonable to conclude that the observed behavior corresponds to the intrinsic magnetocrystalline anisotropy of $(001)^T$ oriented films, which gives rise to magnetic easy plane in $(001)^T$.

From the measured magnetic hysteresis loops of the 250 Å LCMO films, we have estimated the magnetostriction constant λ and the uniaxial anisotropy constant K_u in order to quantify the stress-induced anisotropy of LCMO films. Standard expressions for the stress-induced anisotropy field $H_{\rm an}=3\lambda\sigma/M_S$ and $K_u=3\lambda\sigma/2$[11] were used with σ the biaxial stress in the film, and H_s along magnetic hard axes were assumed to be approximately equal to $H_{\rm an}$. In the 250 Å LCMO film grown on LAO the observed -0.99% in-plane biaxial compressive strain corresponds to a compressive stress of about -5×10^{10} dyne/cm^2 using a Young's modulus of 5×10^{12} dyne/cm^2.[12] From this we obtain the respective λ and K_u values to be 1.5×10^{-5} and -1.2×10^6 erg/cm^3. Similarly, the respective values for the 250 Å LCMO film grown on STO, which is under a $+0.74\%$ in-plane tensile strain, are 3×10^{-5} and $+1.8\times10^6$ erg/cm^3. As expected from the above discussion, the negative K_u of the former confirms the presence of a uniaxial easy axis, and the positive value of the latter confirms an easy plane. The presence of a positive magnetostriction in the LCMO films is also confirmed by this estimate. Comparable magnetostriction and uniaxial anisotropy constants were found in LCMO films grown by molecular beam epitaxy,[5] in *Y*-doped LCMO films,[13] and in $La_{0.7}Sr_{0.3}MnO_3$ films[4] in which K_u was deduced from torque magnetometer measurements.

In summary, we have studied the effect of 3D strain states on magnetic anisotropy of epitaxial LCMO films grown on two types of (001) substrates, $SrTiO_3$. and $LaAlO_3$ Our x-ray results indicate unambiguously that the two types of substrates lead to the formation of two corresponding domain structures in the LCMO films. We show that the magnetic anisotropy of strained LCMO epitaxial films correlates strongly with the nature of the substrate-induced 3D strain states, such that the magnetic easy axis is along the direction of tensile strain, indicating the presence of a positive magnetostriction. Strain relaxation in the thicker films leads to the formation of both $(001)^T$ and $(110)^T$ oriented grains, and the corresponding magnetic easy axis lies in the film plane along the [110] direction of the substrate.

This work was supported by the David and Lucile Packard Fellowship (CBE), the NSF Young Investigator Award (CBE), ONR Grant No. N00014-95-1-0513, and NSF Grant No. DMR 9802444. F.T. acknowledges support from NSF Grant Nos. DMR 9703419 and DMR 9601825.

[1] S. Jin, T. H. Tiefel, M. McCormack, R. A. Fastnacht, R. Ramesh, and L. H. Chen, Science **264**, 413 (1994); S. Jin, T. H. Tiefel, M. McCormack, H. M. O'Bryan, L. H. Chen, R. Ramesh, and D. Schurig, Appl. Phys. Lett. **67**, 557 (1995).
[2] Q. Gan, C. B. Eom, L. Wu, and F. Tsui (in press).
[3] G. Cao, S. McCall, M. Shepard, J. E. Crow, and R. P. Guertin, Phys. Rev. B **56**, 321 (1997),
[4] Y. Suzuki, H. Y. Hwang, S.-W. Cheong, and R. B. van Dover, Appl. Phys. Lett. **71**, 140 (1997).
[5] J. O'Donnell, M. S. Rzchowski, J. N. Eckstein, and I. Bozovic, Appl. Phys. Lett. **72**, 1775 (1998).
[6] C. Kwon, M. C. Robson, K.-C. Kim, J. Y. Gu, S. E. Lofland, S. M. Bhagat, Z. Trajanovic, M. Rajeswari, T. Venkatesan, A. R. Kratz, R. D. Gomez, and R. Ramesh, J. Magn. Magn. Mater. **172**, 229 (1997).
[7] S. Jin, M. McCormack, T. H. Tiefel, and R. Ramesh, J. Appl. Phys. **76**, 6929 (1994).
[8] M. T. Johnson, P. J. H. Bloemen, F. J. A. den Broeder, and J. J. Vries, Rep. Prog. Phys. **59**, 1409 (1996).
[9] C. B. Eom, R. J. Cava, R. M. Fleming, J. M. Philips, R. B. van Dover, J. H. Marshall, J. W. P. Hsu, J. J. Krajewski, and W. F. Peck, Jr., Science **258**, 1766 (1992).
[10] R. A. Rao, D. Lavric, T. K. Nath, C. B. Eom, L. Wu, and F. Tsui, Appl. Phys. Lett. **73**, 3294 (1998).
[11] B. D. Cullity, *Introduction to Magnetic Materials* (Addison–Wesley, Reading, MA, 1972), p. 268.
[12] *American Institute of Physics Handbook*, edited by D. E. Gray (McGraw–Hill, New York, 1972), pp. 3–126.
[13] M. R. Ibarra, P. A. Algarabel, C. Marquina, J. Blasco, and J. Garcia, Phys. Rev. Lett. **75**, 3541 (1995).